Journal of Applied Electrochemistry **34**: 403–408, 2004.

Metallic-lithium, $LiFePO_4$-based polymer battery using PEO–ZrO_2 nanocomposite polymer electrolyte

A. D'EPIFANIO[1,2], F. SERRAINO FIORY[2], S. LICOCCIA[2], E. TRAVERSA[2], B. SCROSATI[1] and F. CROCE[3,*]
[1]*Department of Chemistry, University of Rome "La Sapienza", Italy*
[2]*Department of Chemical Science and Technology, University of Rome "Tor Vergata", Italy*
[3]*Dipartimento di Scienze del Farmaco, Università degli Studi "G. D'Annunzio", 66013, Chieti, Italy*
*(*author for correspondence, e-mail: fausto.croce@unich.it)*

Received 21 July 2003; accepted in revised form 4 November 2003

Key words: lithium polymer battery, PEO-based polymer electrolyte, ZrO_2 filler

Abstract

A study of the electrochemical properties of a PEO-based polymer electrolyte with nanometric ZrO_2 as ceramic filler has been carried out in order to confirm an earlier reported model dealing with the role of ceramic fillers within PEO-based polymer electrolytes as components that enhance such properties as conductivity, lithium transference number, compatibility with lithium metal electrodes and cyclability. A prototype of a lithium polymer battery, based on a membrane made from a nanocomposite polymer electrolyte doped with ZrO_2, utilizing $LiFePO_4$ + 1%Ag as cathode, has been assembled and galvanostatically cycled, resulting in excellent performance at temperatures ranging from 100 °C to 60 °C (close to the crystallization temperature of PEO).

1. Introduction

In previous works [1, 4] we have illustrated and discussed the transport properties of various types of nanocomposite polymer electrolytes formed by dispersing selected types of ceramic powders having nanoparticle sizes into a PEO–LiX matrix. The electrochemical investigation of these materials has clearly demonstrated that the ceramic fillers induce relevant effects, such as a consistent enhancement of the ionic conductivity, both below and above the PEO crystallization temperature, a consistent enhancement of the lithium transference number, and an improvement in terms of capability and cyclability of PEO based nanocomposite polymer electrolyte lithium batteries [5].

These effects have been interpreted assuming a specific role of the ceramic filler particles that is not limited to the sole action of preventing crystallization of the polymer chains, but also, and in particular, to promote specific interactions between the particle surface groups and both the PEO segments and the electrolyte ionic species. It is possible to explain the effects caused by the presence of the ceramic filler by assuming an enhancement of salt dissociation and a stabilization of the amorphous phase in the polymer matrix. Both these phenomena have been attributed to acid–base Lewis type ceramic–electrolyte interactions between the polar surface groups of the inorganic filler and the electrolyte ionic species [6].

Previously [7], we have shown that the interactions of the –OH groups present on the surface of the Al_2O_3 dispersoids lead to enhanced behaviour of the polymer electrolyte via the following three basic mechanisms.

(i) Decreasing the salt association (which is severe in a very low dielectric media like PEO) by an 'hydrogen-bond-mediated' solvation of the anions due to the –OH groups present on the surface of the inorganic particles, according to the following scheme:

$$LiX + Al_2O_3(OH)_{surface} \rightleftharpoons Li^+ + X^- - (HO - Al_2O_3)$$

The inorganic filler may be regarded as an 'anionic solvent'.

(ii) Freeing the Li^+ cations from the PEO chain helical coordination due to hydrogen bond interactions between the oxygen atoms of the polymer and the surface groups of dispersoids, according to the scheme shown in Figure 1.

(iii) Formation of hydrogen-bond mediated interchains cross-linking according to Figure 2.

As a consequence, in the first process an increase in the number of charge-carriers (due to the decrease in salt association) and a decrease in the anionic mobility due to the surface OH-groups mediated anionic salvation is expected. The predicted effects on the macroscopic properties of the polymer electrolyte are higher ionic conductivity, both in the amorphous and crystalline

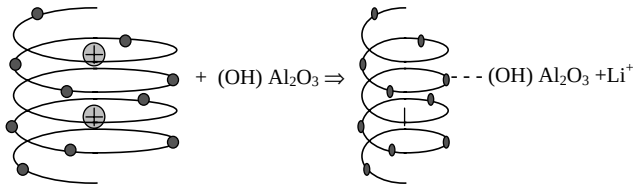

Fig. 1. Schematic representation of PEO-chain Al_2O_3 surface group interaction.

regions of the electrolyte, and higher cationic transference number. The second process, also, leads to an increase in the charge carrier concentration and should produce higher ionic conductivities above and below the PEO melting temperatures. Finally, the third process has the effect of lowering the PEO crystallization kinetics thus stabilizing the more conductive amorphous phase at temperatures below the polymer crystallization temperature.

For the case of nanocomposite polymer electrolytes having the composition $(PEO)_{20}LiCF_3SO_3$ + 10% acidic-Al_2O_3 we have experimentally demonstrated the occurrence of all the beneficial effects on the macroscopic properties predicted by the hydrogen bond-mediated, oxide-surface-OH-group/polymer-electrolyte-component interaction model [1–4, 8]. Furthermore, we have found an improvement in terms of capability and cyclability of PEO-based nanocomposite polymer electrolyte lithium batteries [5].

To confirm these hypotheses we have here studied the system formed by dispersing nano-sized particles of ZrO_2, a compound well known in the literature for having strong Lewis acid groups on its surface, in a PEO based solid polymer electrolyte. This nanocomposite system is expected to behave as a superior polymer electrolyte for high-performance lithium metal rechargeable battery as it should have all the beneficial features previously found for PEO-based acid-Al_2O_3 composites without the drawbacks of poor chemical stability toward the metallic lithium, this latter being due to the presence of the very reactive OH groups on the Al_2O_3 surface. Moreover, we have assembled a prototype of lithium metal rechargeable battery with the new cathodic material $LiFePO_4$ + 1% Ag [9] whose features have been demonstrated to be compatible with the working conditions of PEO based polymer electrolytes.

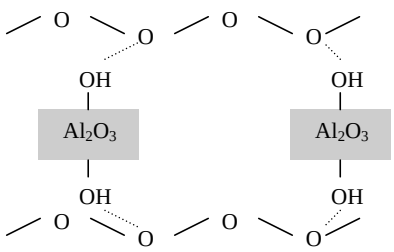

Fig. 2. Schematic representation of cross-link formation.

2. Experimental details

The zirconia ceramic filler was prepared by hydrolysis of zirconium isopropoxide at ambient temperature in aqueous alcoholic solution. The procedure was as follows: an ethanol solution of $Zr(OiPr)_4$ was added drop wise to a solution of ethanol/water 1:1 under rapid stirring. The suspension obtained was stirred for 10 min, then filtered giving a white precipitate that was dried in air (110 °C) for 15 h in order to allow water removal and then heated at 500 °C for 2 h. The powder so obtained was milled for 2 h. The calcination temperature was selected according to the thermal analysis results. Simultaneous thermogravimetric/differential thermal analysis (TG/DTA) was performed by a thermoanalyser (STA 409, Netzsch) in air flow (1.33 $cm^3\ s^{-1}$) using a heating rate of 0.16 °C s^{-1} over a 25–900 °C temperature range. The morphology and the mean particle diameters were determined by scanning electron microscopy (SEM) of the powders.

The nanocomposite polymer electrolyte was obtained by mixing PEO 600.000 (Aldrich) with $LiCF_3SO_3$ (Fluka, purum) and ZrO_2 nanometric powder. The $LiCF_3SO_3$–PEO concentration ratio was fixed at 1/20 and the amount of added ceramic at 10% of the total PEO_{20}-$LiCF_3SO_3$ weight. The ceramic filler, the lithium salt and the polymer were dispersed in acetonitrile. The slurry obtained by mixing the components was then cast onto a Teflon plate and the solvent allowed to evaporate slowly at room temperature by trapping it into molecular sieves. The resulting membrane (average thickness 100 μm) was dried under vacuum at 45–50 °C for 24 h [6].

The impedance spectroscopy of the membrane was carried out by measuring the response of cells formed by sandwiching the given electrolyte membrane sample between two polished stainless steel electrodes in the 1 Hz–100 kHz frequency range. A Solartron (model 1260) potentiostat coupled with a 1255 FRA (frequency response analyser) was used to run all the impedance tests. The lithium ion transference number, T_+ was evaluated using the method proposed by Jacobsen and Sorensen [10]. Accordingly, the T_+ values were determined by studying the impedance spectra in the 1 mHz–100 kHz frequency range, of a Li/electrolyte sample/Li cell. The Li–polymer electrolyte compatibility was evaluated by studying the time evolution of the impedance spectra in the 1 Hz– 100 kHz frequency range of a similar cell.

The metallic-Li complete cell was assembled by sandwiching a lithium foil as anode, the nanocomposite polymeric membrane as electrolyte, and a film-type $LiFePO_4$ active material (83%) with 1 wt % of silver, mixed with a carbon (M.M.M. Carbon Belgium Super P, 12 wt %) conductive additive and a PVdF (Solvay Solef 6020, 5 wt %) binder, as cathode.

The galvanostatic cycling test was carried out at different temperatures using a Maccor battery tester and by setting the charge cut-off voltage at 3.8 V and the discharge cut-off voltage at 3.0 V.

3. Results and discussion

Figure 3 shows the TG/DTA scan of the ZrO_2. The TG curve shows a weight loss of 14% from room temperature to 400 °C probably due to the loss of water and alcohol. The DTA scan shows a sharp and intense exothermic peak with a maximum at about 420 °C due to the decomposition and combustion of residual organic groups. No weight loss was observed over 450 °C. Therefore, it was decided to thermally treat the powder precursors at 500 °C for 2 h to synthesize the final compound.

The SEM image of Figure 4 clearly shows that the particles of ZrO_2 have average diameters of about 30–40 nm.

We tested the electrochemical behaviour of the nanocomposite polymer electrolyte in comparison with the behaviour of the sample without ceramic filler. Figure 5 reports the Arrhenius trace of the PEO-based electrolyte with added ZrO_2 compared to that of the plain polymer. It can be seen that a significant enhancement of the composite sample conductivity occurs both above and below 60 °C (the PEO crystallization temperature).

The lithium ion mobility was evaluated by the transference number using the well-known Jacobsen–Sorensen formula:

$$T_+ = \frac{R_{\text{bulk}}}{(R_{\text{bulk}} + Z_{\text{diff}})}$$

Figure 6 reports a typical impedance spectrum of a symmetrical non-blocking cell using two metallic lithium electrodes in contact with the polymeric electrolyte under test. The trace shows all the features which characterize the mass and charge transport processes through the cell: namely, (i) a high frequency real-axis intercept commonly assigned to the bulk electrolyte resistance; (ii) a middle frequency semicircular dispersion associated to the charge transfer resistance, which originates at the interfaces of both the electrodes with the electrolyte, in parallel with the double layer capacitance; (iii) a low frequency 45° slope linear spike pointing toward the real axis at lowest frequencies, as expected for a thin-layer diffusion at non-blocking electrodes [7].

The T_+ value found at 85 °C was 0.42, showing an increase with respect to that of the ceramic-free sample (previously found to be 0.27). This behaviour also

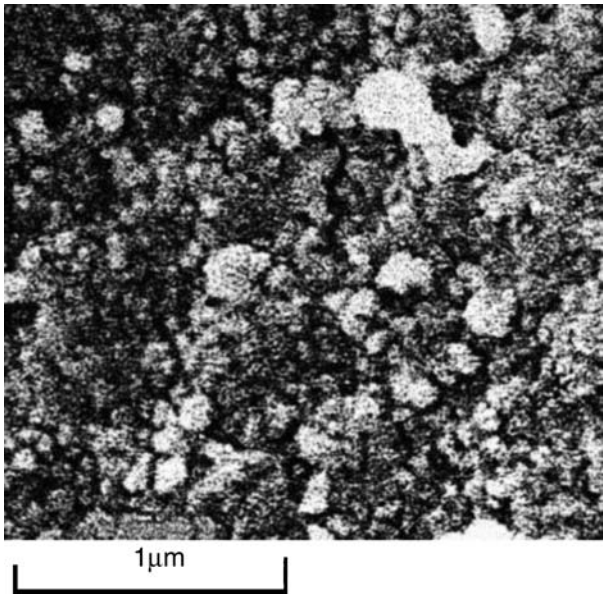

Fig. 4. SEM image of ZrO_2 powder prepared by sol–gel technique at 500 °C.

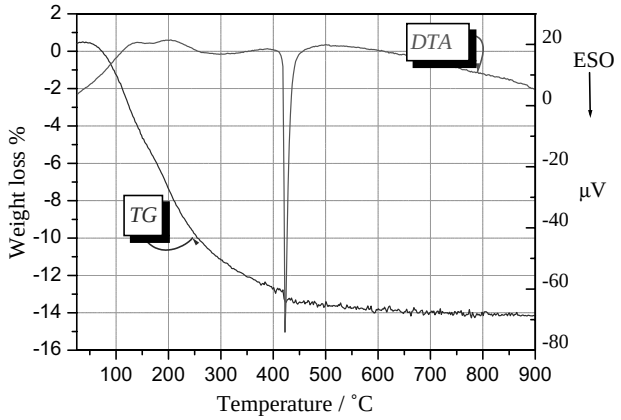

Fig. 3. TG and DTA scans of the ceramic filler before the thermal treatment at 500 °C.

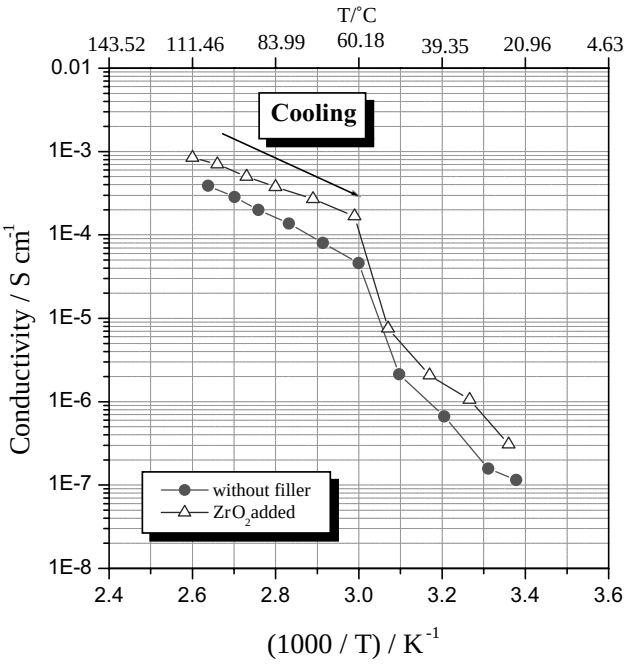

Fig. 5. Arrhenius plot of conductivity of $P(EO)_{20}LiCF_3SO_3$ + 10w/o ZrO_2 composite polymer electrolyte. The conductivity of a $P(EO)_{20}$-$LiCF_3SO_3$ ceramic-free sample is also reported for comparison purposes. Data obtained by impedance measurements.

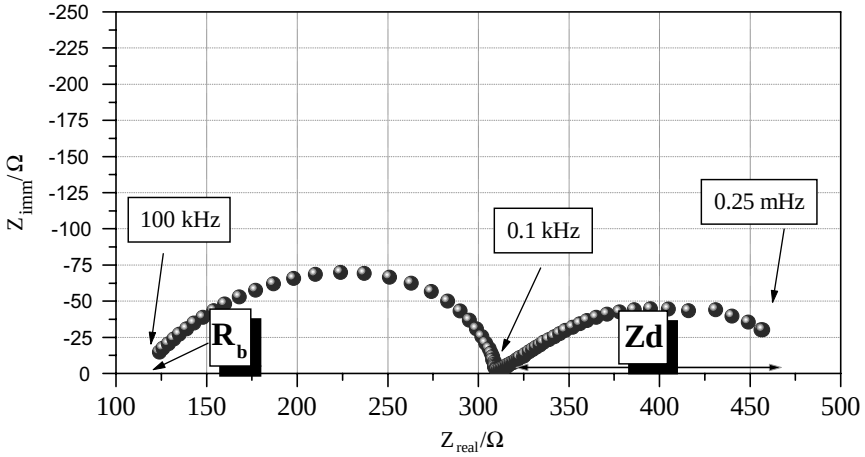

Fig. 6. Determination of lithium ion transference number of Li | $P(EO)_{20}LiCF_3SO_3$ + 10w/o ZrO_2 | Li cell, $T = 85$ °C. Measurements according to the method proposed by Jacobsen–Sorensen.

confirms the model developed by Croce and coworkers [6, 8].

In previous papers [2, 6, 8] we have demonstrated that the structural modifications induced by the ceramic filler are more effective according to the acidity of the particle surface, so, the acidic-Al_2O_3, whose surface is covered by –OH groups, has better electrochemical properties (conductivity, transference number) than the neutral-Al_2O_3. These improvements in transport properties have the consequence of a lower stability of the interface lithium–nanocomposite polymer electrolyte, as the –OH groups are expected to be very reactive with the metallic lithium. To check this latter hypothesis we compared the time evolution of the impedance of the cell:

$$\mathrm{Li}\,|\,\mathrm{P(EO)_{20}LiCF_3SO_3} + 10\ \mathrm{wt\ \%\ ZrO_2}\,|\,\mathrm{Li}$$

against that of the cells:

$$\mathrm{Li}\,|\,\mathrm{P(EO)_{20}LiCF_3SO_3} + 10\ \mathrm{wt\ \%\ neutral - Al_2O_3}\,|\,\mathrm{Li}$$

and

$$\mathrm{Li}\,|\,\mathrm{P(EO)_{20}LiCF_3SO_3} + 10\ \mathrm{wt\ \%\ acidic - Al_2O_3}\,|\,\mathrm{Li}$$

By analysing the spectra it has been possible to separate the contributions to the overall lithium–polymer electrolyte interface impedance of both the passivation layer resistance itself and of the charge transfer resistance. All the measurements were taken at 90 °C in order to minimize any possible grain boundary effects which are present when the amorphous and crystalline phases coexist below 60 °C [1].

As can be clearly seen in Figure 7, the sample containing acidic-Al_2O_3 shows the highest value of the passivation layer resistance coupled with a marked instability during all the measuring period. In contrast, electrolyte samples containing respectively neutral-Al_2O_3 and ZrO_2 showed a similar behaviour: a very stable interface coupled to limited resistance values. These results can be explained by taking into account the superficial properties of the powders: the acidic-Al_2O_3 surface is almost entirely covered by –OH groups which can react easily with the metallic lithium electrode surface forming thick, highly resistive passivation layers

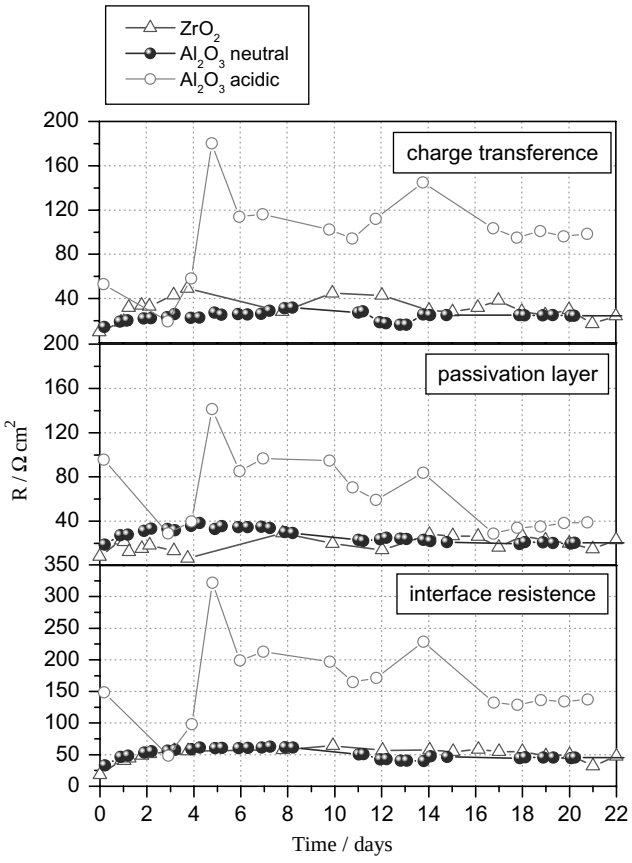

Fig. 7. Time evolution of the interfacial parameters of Li | $P(EO)_{20}$-$LiCF_3SO_3$ + 10w/o ceramic filler nanocomposite polymer electrolyte interface at $T = 90$ °C.

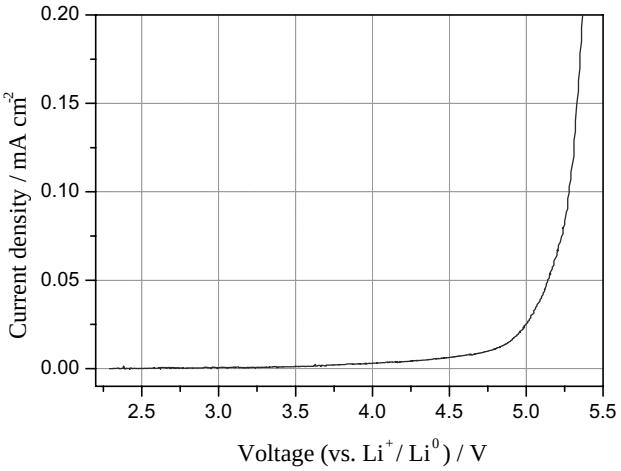

Fig. 8. Anodic sweep of Li | $P(EO)_{20}LiCF_3SO_3$ + 10w/o ZrO_2 | SS cell; $T = 85$ °C, scan-rate = 200 μV s^{-1}.

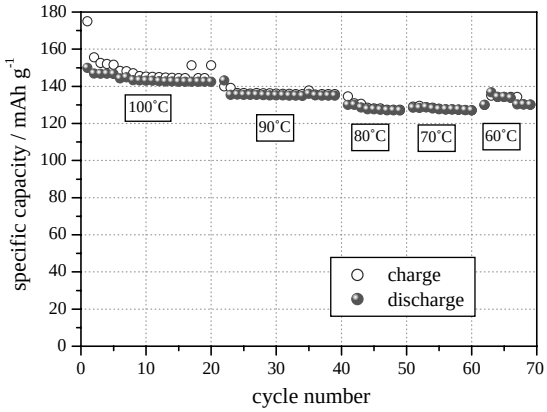

Fig. 9. Galvanostatic cycling test of $LiFePO_4$ + 1%Ag | P(EO) $20LiCF_3SO_3$ + 10w/o $ZrO_2$2 | Li at different temperature.

[2], which, in turn, hinder the charge transfer process at the interface (as evidenced by the charge transfer resistance traces reported in Figure 7). This phenomenon is well known for being responsible for the poor performance of metallic-lithium polymeric batteries in terms of cyclability.

The idea of using ZrO_2 as ceramic filler was to obtain all the advantages of having strong Lewis-acid particle surfaces without the presence of –OH groups (as the thermal traces of Figure 3 show). This should result in electrolytes with improved conductivity and transference number values, similar to those seen for the sample containing acidic-Al_2O_3, together with better metallic-lithium interface stability as seen in Figure 7 for the samples containing (neutral and basic)-Al_2O_3.

Finally, to further qualify this polymeric electrolyte, the decomposition voltage of the nanocomposite PEO based membrane was evaluated by running sweep voltammetry on a cell having the configuration: *lithium | polymer electrolyte | stainless steel*. The results are shown in Figure 8. Two main favourable features are seen in this Figure, namely:

(i) The onset of the current is detected around 4.2 V vs Li^+ | Li^o half cell; this value is assumed as the membrane anodic breakdown voltage. This voltage is high enough for a safe use of the membrane in connection with the $LiFePO_4$ + 1% Ag cathode which, typically, cycles around 3.5 V.

(ii) The residual current prior to the break-down is extremely small, giving clear evidence of the high purity of the membrane.

Figure 9 shows the cycle performance of a cell having the configuration:

$$Li|P(EO)_{20}LiCF_3SO_3 + 10\ w/o\ ZrO_2|LiFePO_4 + 1\%Ag$$

operated at 100, 90, 80, 70 and 60 °C. The capacity of the cell increased as the operating temperature was raised and there was no significant capacity loss over the whole temperature range. These data indicate that the lithium diffusion in $LiFePO_4$ + 1% Ag is enhanced as the temperature increases [11, 12].

Moreover, it is evident how this nanocomposite polymer electrolyte can function with good performance, in terms of capacity, at temperature as low as 60 °C which is beyond the crystallization temperature of conventional polymer electrolytes.

4. Conclusions

A previous developed model in which we attributed an increase in electrochemical properties of nanocomposite PEO based polymer electrolytes to the superficial acidity of the ceramic powders dispersed in the polymeric matrix, which promoted specific interactions between the fillers, the polymeric chains and the ions coming from the salt dissociation, has been confirmed. Furthermore, we have obtained substantial improvement in the performances of an electrochemical device based on this electrolyte, which makes use of nanosized ceramic fillers having a high Lewis-type surface acidity. These properties make the $P(EO)_{20}LiCF_3SO_3$ + 10w/o ZrO_2 composite polymer electrolyte a very promising material for the development of an efficient rechargeable lithium polymer battery able to work near the crystallization temperature of the polymer. In fact, in this paper we have demonstrated that a lithium-metal rechargeable battery utilizing $P(EO)_{20}LiCF_3SO_3$ + 10w/o ZrO_2 as electrolyte and $LiFePO_4$ + 1% Ag as cathode has features, in terms of high power capability at low temperatures, largely exceeding those so far reported for other more conventional types of lithium polymer batteries utilizing other nanocomposite polymer electrolytes.

References

1. F. Croce, G.B. Appetecchi, L. Persi and B. Scrosati, *Nature* **394** (1998) 456.

2. F. Croce, R. Curini, A. Martinelli, L. Persi, F. Ronci, B. Scrosati and R. Caminiti, *J. Phys. Chem. B* **103** (1999) 10632.
3. B. Scrosati, F. Croce and L. Persi, *J. Electrochem. Soc.* **5** (2000) 1718.
4. G.B. Appetecchi, F. Croce, L. Persi, F. Ronci and B. Scrosati, *Electrochim. Acta* **45** (2000) 1481.
5. F. Croce, F. Serraino Fiory, L. Persi and B. Scrosati, *Electrochem Solid State Lett.* **4** (2001) A121.
6. F. Croce, L. Persi, B. Scrosati, F. Serraino Fiory, E. Plichta and M.A. Hendrickson, *Electrochim. Acta* **46** (2001) 2457–2461.
7. J. Ross MacDonald and W.R. Kenan, 'Impedance Spectroscopy: Emphasizing Solid Materials and Systems' (J. Wiley & Sons, New York, 1987).
8. F. Croce and B. Scrosati, *Ann. N.Y. Acad. Sci.* **984** (2003) 1.
9. F. Croce, A. D'Epifanio, A. Deptula, W. Lada, J. Hassoun and B. Scrosati, *Electrochem. Solid State Lett.* **5** (2002) A47.
10. P.R. Sorensen and T. Jacobsen, *Electrochim. Acta* **27** (1982) 1671.
11. A.K. Padhi, K.S. Nanjundaswami and J.B. Goodenough, *J. Electrochem. Soc.* **144** (1997) 1188.
12. Masaya Takahashi, Shinichi Tobishima, Koji Takei and Yoji Sakurai, *J. Power Sources* **97–98** (2001) 508.